Assessment of ocean colour remote sensing photosynthetically available radiation in the Southeastern Brazilian margin

João Felipe Cardoso dos Santos[1]
Milton Kampel[1]

[1]Instituto Nacional de Pesquisas Espaciais - INPE
Caixa Postal 515 - 12227-010 - São José dos Campos - SP, Brasil
{joaofcs, milton}@dsr.inpe.br

Abstract. Photosynthetically available radiation (PAR) comprises the integrated irradiance between 400–700 nm which reaches the sea surface. Its importance in the marine environment is directly related to primary productivity, which uses light in the atmospheric carbon assimilation reactions. The algorithm for estimating PAR with Sea-viewing Wide Field-of-View Sensor (SeaWiFS) data was evaluated in relation to *in situ* measurements during the summer and winter of 2001 and 2002. Estimates showed a mean RMSE of ~1.77 Einstein m^{-2} d^{-1} and bias ~1.63 Einstein m^{-2} d^{-1} for the complete dataset (summer + winter). A generalized linear model (GLM) was applied to the complete dataset decreasing the RMSE values for < 0.7 Einstein m^{-2} d^{-1} and bias approaching zero. PAR estimates with SeaWiFS, MODerate Imaging Spectroradiometer (MODIS-*Aqua*) and MEdium Resolution Imaging Spectrometer (MERIS) data were also compared during the winter of 2002. All three satellite estimates overestimated the *in situ* measurements with a bias of ~1.5 Einstein m^{-2} d^{-1}. Statistical analyzes (RMSE, bias and r2) indicated a systematic error corrected by GLM. After the adjustments, the estimates showed values of bias close to zero and lower RMSE. The best performance was observed with MODIS-*Aqua* data followed by SeaWiFS and MERIS, consecutively. In general, the estimations of PAR showed a good correlation with the *in situ* measurements and the linear adjustments corrected the observed systematic error making possible its application to other ocean colour sensors in operation.

Keywords: sea surface irradiance, SeaWiFS, MODIS, MERIS, generalized linear model, irradiância na superfície do mar, SeaWiFS, MODIS, MERIS, modelo linear generalizado.

1. Introduction

Photosynthetically available radiation (PAR) refers to radiation with wavelengths between 400 and 700 nm (FROUIN et al., 2012). It is fundamental to most ecological and biophysical processes because it plays a key role in energy balance on a local and global scale. In the oceanic environment monitoring of PAR is important for modeling heat fluxes within the surface layer (FROUIN et al., 2012; KAWAI; WADA, 2007). The heat flux, consequently, may vary the sea surface temperature (SST) during the day, so called diurnal SST variation (GENTEMANN et al., 2003). The diurnal variation could be related with meteo-oceanographic process and modify the mixed-layer deepening/shoaling (DENMAN et al., 1973; KAWAI; WADA, 2007). Biologically the PAR can affect the phytoplankton distribution along the water column considering that the availability of light energy tends to be smaller with increasing depth (PEREIRA; SOARES-GOMES, 2002). Estimation of daily PAR (Einstein m^{-2} d^{-1}) from ocean colour remote sensing is also important for monitoring the oceanic primary productivity and the subsequent assimilation of carbon by phytoplankton in the photosynthesis process (HARMEL; CHAMI, 2016).

Photosynthesis is the biological conversion of dissolved inorganic carbon in organic molecules of high energy (FALKOWNSKI et al., 2003; FALKOWSKI; RAVEN, 2007; SIGMAN; HAIN, 2012) and is controlled by the availability in nutrients within the water column (e.g., nitrate, phosphate, iron) and by the amount of light entering the ocean. The quantity of carbon resulting from the integration of photosynthesis over a certain time and area is called primary productivity (PP) and is usually expressed as gC m^{-2} d^{-1} (ANTOINE, 2006). The primary productivity is also limited by weather factors such as cloud cover and airborne particles influence the degree of incidence of light on the surface of the ocean and can reduce the availability of light for the phytoplankton, regardless of the sea conditions (PEREIRA; SOARES-GOMES, 2002).

Accurate estimation of daily PAR from satellite observations is therefore a prerequisite to provide a global coverage of biogeochemical parameters such as the ocean PP (HARMEL; CHAMI, 2016). At least 90% accuracy of daily PAR is useful for modeling oceanic PP (FROUIN; PINKER, 1995). This study aims to evaluate ocean colour remote sensing estimate of PAR in the Southeastern margin of Brazil and validate adjustments of a regional model applied to data from different ocean colour sensors during summer and winter of 2001 and 2002.

2. Methodology

The study area correspond to the north portion of the Brazilian Southeastern continental margin delimited between Cape of São Tomé (ST), in Rio de Janeiro state (22°S), and São Sebastião Island (SSI), in São Paulo state (24°S) (Figure 1). The *in situ* data were obtained during mesoscale cruises of the project *Dinâmica do Ecossistema de Plataforma da Região Oeste do Atlântico Sul* (DEPROAS) in summer (February) and winter (July) of 2001 and repeated in summer (January) and winter (August) of 2002. *In situ* data were acquired by a quantum scalar surface reference sensor QSR-240 (*Biospherical Instruments Inc.*) equally sensitive to photons from all direction measures in the interval between 400–700 nm. Due to technical problems some *in situ* data were invalid. To solve this problem we utilized a spectral irradiance model as described by Bird (1984) to determine the available energy in the sea surface, validated with the *in situ* measurements. The total irradiance $I_0(t)$ (Watt m^{-2}) was calculated as a function of time (t, hours), geographic position (latitude) according to the ship coordinates, *in situ* measurements of cloud cover observed during the cruises, day length (hours) and day of the year (Julian calendar). Some adjustments were applied for seasonal variations as suggested by Sathyendranath and Platt (1988). Details of these *in situ* PAR data were described by Kampel (2003).

Level 1 Sea-viewing Wide Field-of-View Sensor (SeaWiFS) sensor, MODerate Imaging Spectroradiometer (MODIS-*Aqua*) and the MEdium Resolution Imaging Spectrometer (MERIS) daily images were acquired during DEPROAS campaigns from the OceanColor Web page (http://oceancolor.gsfc.nasa.gov/cms/) and processed to Level 2 using the SeaWiFS Data Analysis System (SeaDAS) version 7.3. Level 2 images were reprojected to the geographic coordinate system *datum* World Geodetic System 1984 (WGS84), preserving the nominal spatial resolution of 1 km. When two or more images of the same sensor on the same day were available an average composite was generated from overlaid pixels. The study area was defined in terms of latitudes 20°S – 26°S and longitudes 40°O – 46°O (Figure 1).

The atmospheric correction algorithm applied was based on the Equation 1 described in detail by Mobley et al. (2016):

$$L_t(\lambda)=\left[L_r(\lambda)+L_a(\lambda)+t_{dy}(\lambda)*L_f(\lambda)+t_{dy}(\lambda)*L_w(\lambda)\right]*t_{gy}(\lambda)*t_{gs}(\lambda)*f_p(\lambda) \quad (1)$$

Where $L_t(\lambda)$ is the radiance signal observed by the satellite after the interaction with the ocean and atmosphere, $L_r(\lambda)$ is the contribution from the Rayleigh molecular scattering, $L_a(\lambda)$ is the contribution due to aerosol scattering, $L_f(\lambda)$ is the contribution by *whitecaps* and the sea surface foam and $L_w(\lambda)$ is the contribution from the upward water radiation. The term $t_{dy}(\lambda)$ represents the transmittance from diffuse radiation trough the optical trajectory from ocean to sensor, $t_{gy}(\lambda)$ e $t_{gs}(\lambda)$ are the transmittance losses by absorption gasses over the sun to the ocean and the ocean to the sensor path, respectively. Finally, $f_p(\lambda)$ is the polarization adjustment.

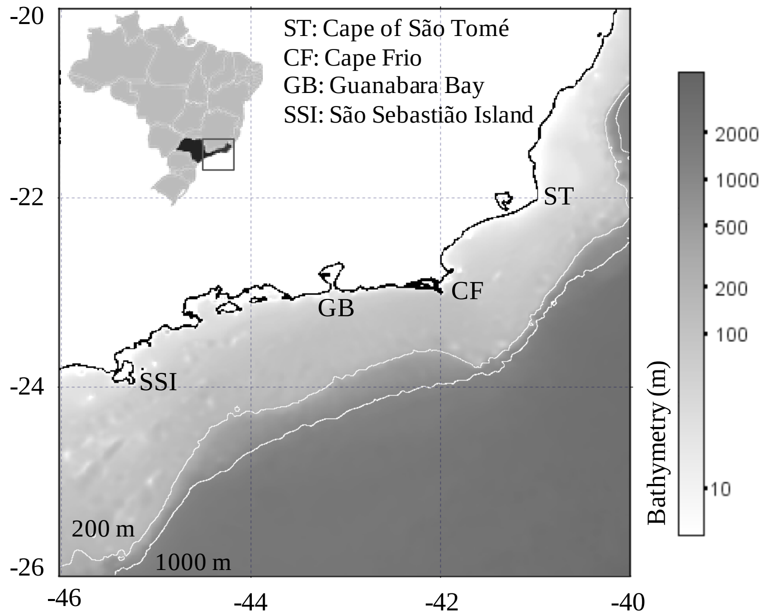

Figure 1. Study area localized in the northern portion of the Brazilian Southeastern continental margin. The white lines correspond to 200 m and 1000 m isobaths (depths are in shades of grey).

Ocean colour remote sensing (OCRS) estimation of PAR (Einstein m^{-2} d^{-1}) was derived from the solar irradiance (E_s, mW cm^{-2} μm^{-1}) integrated in the visible range of the electromagnetic radiation (400-700 nm) over the day length defined by latitude and date of acquisition (FROUIN et al., 2003). The implementation of this algorithm (Equation 2) depends on the availability of the irradiance at the top of the atmosphere limited by saturation clouds:

$$PAR(400\text{-}700) = \int_{\lambda=400}^{\lambda=700} E_d(\lambda) d\lambda = \frac{E_s(1\text{-}A)}{(1\text{-}A_s)*(1\text{-}S_a A)} \qquad (2)$$

Where $E_d(\lambda)$ (mW cm^{-2} μm^{-1}) is the downward irradiance after the interaction with atmosphere, S_a refers to the spherical albedo, A is the albedo of clouds and aerosols on cloud-surface path and can be reduced to S_a when in ideal weather conditions. E_s is the solar irradiance that should reach the sea surface if A did not exist (ZEGE et al., 1991). At the end of the process, the PAR is obtained in units of mW cm^{-2} μm^{-1} and converted to Einstein m^{-2} d^{-1} by a factor of 1.193 with a small percentage of error regardless of weather conditions (KIRK, 1994). Frouin et al. (2003, 2012) and Frouin and Pinker (1995) provide more details of this algorithm.

Algorithm performance was assessed using the coefficient of determination (r^2), root mean square error (RMSE) and the average error (bias). The criteria for better performance are based on the RMSE, bias and r^2, in this sequence, as suggested by IOCCG (2007). A box plot chart where values below $\{Q_1\text{-}1.5(Q_3\text{-}Q_1)\}$ and above $\{Q_3+1.5(Q_3\text{-}Q_1)\}$ are identified as outliers and then, are removed before the algorithm assessment. Q_1 and Q_3 are the first and third quartiles, respectively.

ISBN: 978-85-17-00088-1

3. Results and Discussion

3.1. Assessment of SeaWiFS data: summer and winter of 2001 and 2002

In general SeaWiFS slightly overestimates the *in situ* values for all 59 concomitant samples with r^2 = 1.0, bias = 1.63 Einstein m^{-2} d^{-1} and RMSE = 1.77 Einstein m^{-2} d^{-1}, that corresponds to ~4.17% higher than the *in situ* values (Figure 2a). Frouin et al. (2012) observed a r^2 = 0.87, bias = 2.83 Einstein m^{-2} d^{-1} and RMSE = 6.49 Einstein m^{-2} d^{-1} for 1,408 samples collected during 2005-2010 at the COVE site off Chesapeak Bay in the North Atlantic. According to these authors the diurnal variability of clouds should be taken into account and may add the bias explained by the time of satellite overpass in the study area. For completely clear sky situations, the PAR estimates from satellite data are in much better agreement with the measurements (FROUIN et al., 2012). Another input error of about 1 Einstein m^{-2} d^{-1} (2 to 3%) is attributed to the accuracy of the irradiance model (FROUIN et al., 2012). Also according to these authors there is a small seasonal variation in the ratio of satellite-derived and measured PAR values.

Frouin et al. (2003) analyzed the estimation of PAR for SeaWiFS data in relation to two moored buoys, one at the relatively high latitude of British Columbia (Halibut Bank, 49°N) and the other in the Equatorial Pacific (0°N). The authors observed a RMSE equal to 6.2 Einstein m^{-2} d^{-1} for both sites and a lower bias in Halibut (0.93) than in Pacific (2.9 Einstein m^{-2} d^{-1}). Despite the performance differences the estimates showed on average a positive bias.

In the present study, the length of the day in the summer campaign was, on average, 13 hours and 12 minutes and during winter 11 hours and 5 minutes. The *in situ* measurements of daily PAR ranged from 58.59 to 62.81 Einstein m^{-2} d^{-1} in the summer season with an average of 60.90 Einstein m^{-2} d^{-1} and between 29.34 to 39.14 Einstein m^{-2} d^{-1} during winter with an average equal to 34.38 Einstein m^{-2} d^{-1}.

During summer, the SeaWiFS algorithm overestimated the *in situ* measurements with bias and RMSE equal to 1.72 and 1.82 Einstein m^{-2} d^{-1}, respectively (Figure 2b). During winter the same algorithm overestimated the *in situ* measurements with bias and RMSE equal to 1.58 and 1.74 Einstein m^{-2} d^{-1}, respectively (Figure 2c). The estimations are above the 90% accuracy of daily PAR for modeling oceanic PP (FROUIN; PINKER, 1995), which can be considered satisfactory. However, both seasons showed a systematic error with similar tendency of overestimation, close values of RMSE and bias and high r^2 (> 0.85). Regional adjustments of a Generalized Linear Model (GLM) allowed the use of a general equation independent of the season (Equation 3):

$$PAR^{*} = 0.99 * PAR_{SeaWiFS} - 1.32 \quad (3)$$

Where PAR^* is the adjusted value. Full analysis of all seasons (summer + winter) presented a r^2 = 1.00, bias = 0.00 and RMSE = 0.68. The previous bias observed for the seasonal analyzes decreased to -0.02 and 0.01 Einstein m^{-2} d^{-1} in the summer and winter, approaching the 1:1 line (Figures 2d,e,f). The results suggested that the systematic error was corrected and the RMSE performance also improved with GLM.

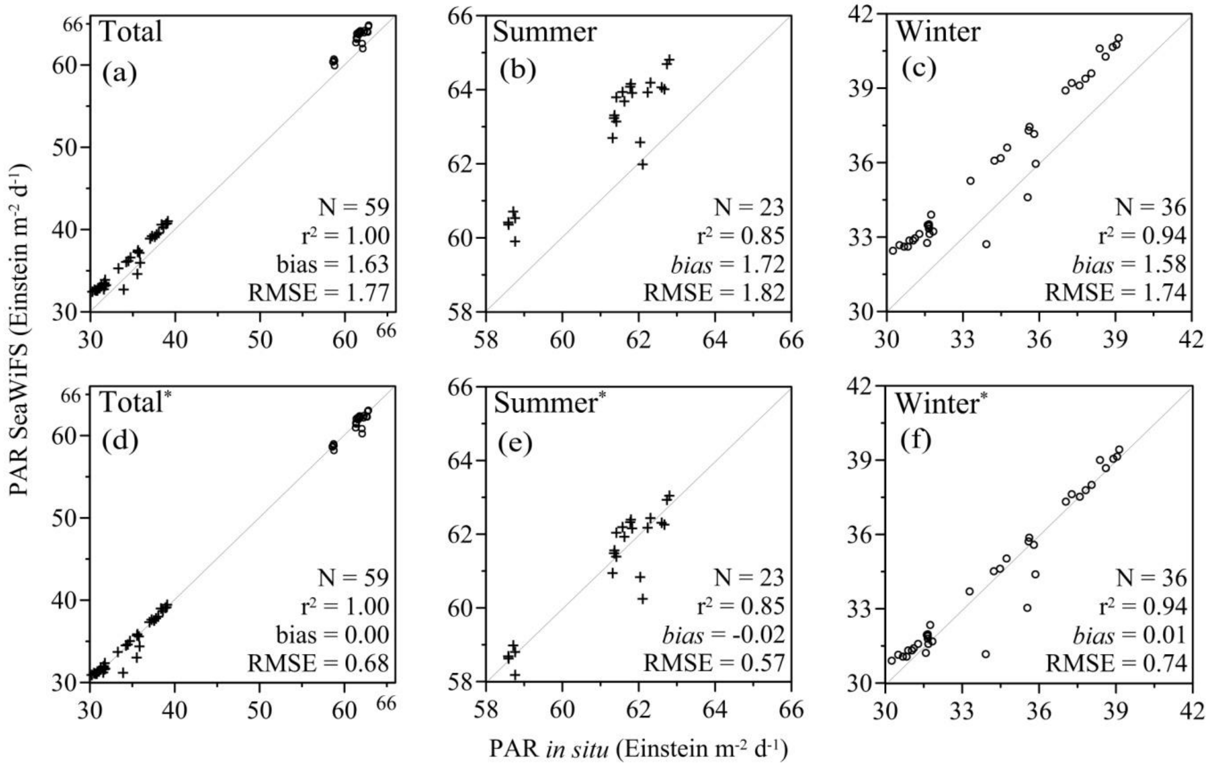

Figure 2. Scatterplots of daily PAR from *in situ* measurements and derived from non-adjusted SeaWiFS data (a, b, c) and adjusted ones (d, e, f).

3.2. Assessment of SeaWiFS, MODIS-*Aqua* and MERIS data: winter of 2002

As MERIS and MODIS-*Aqua* data are only available starting from May and July of 2002, respectively, concomitant daily PAR for the three orbital sensors was possible to obtain only for the winter cruise of 2002. All sensors algorithms overestimated *in situ* measurements. The best performance was obtained with MODIS-*Aqua* data with RMSE = 1.57 (Figure 3b), followed by SeaWiFS with RMSE = 1.67 (Figure 3a) and MERIS with RMSE = 3.06 Einstein m^{-2} d^{-1} (Figure 3c). Main sources of uncertainties are related to cloud cover, seasonal variation and the irradiance model used for *in situ* measurements. Other source of errors may be associated with sensors characteristics and time differences between satellite overpass and *in situ* sampling, also considering changes in atmospheric transmittance and absorption throughout the optical path. SeaWiFS and MODIS-*Aqua* showed similar statistical values (RMSE and bias) and a high r^2. MERIS showed a lower r^2 (0.26) that may be related with two stations that were not considered outliers but underestimated *in situ* data in ~5 Einstein m^{-2} d^{-1}. The GLM was adjusted to all three sensors individually (Equations 4, 5 and 6):

$$PAR^{*}_{SeaWiFS} = 0.73 * PAR_{SeaWiFS} + 8.73 \quad (4)$$

$$PAR^{*}_{MODIS} = 0.97 * PAR_{MODIS} - 0.37 \quad (5)$$

$$PAR^{*}_{MERIS} = 0.32 * PAR_{MERIS} + 24.21 \quad (6)$$

Where PAR^{*} is the adjusted PAR by the GLM for each subscribed sensor. With the regional adjustments the RMSE and bias for SeaWiFS decrease to 0.70 and -0.12 Einstein m^{-2} d^{-1} (Figure 3d), for MODIS-*Aqua* algorithm the RMSE was reduced to 0.34 and the bias was approximately zero (Figure 3e), and for MERIS the RMSE = 1.61 and bias equal to 0.09 Einstein m^{-2} d^{-1} (Figure 3f). These results showed that the GLM was a better choice to correct the systematic errors present on estimates with the three sensors and a simple linear model was able to improve the PAR estimate regionally.

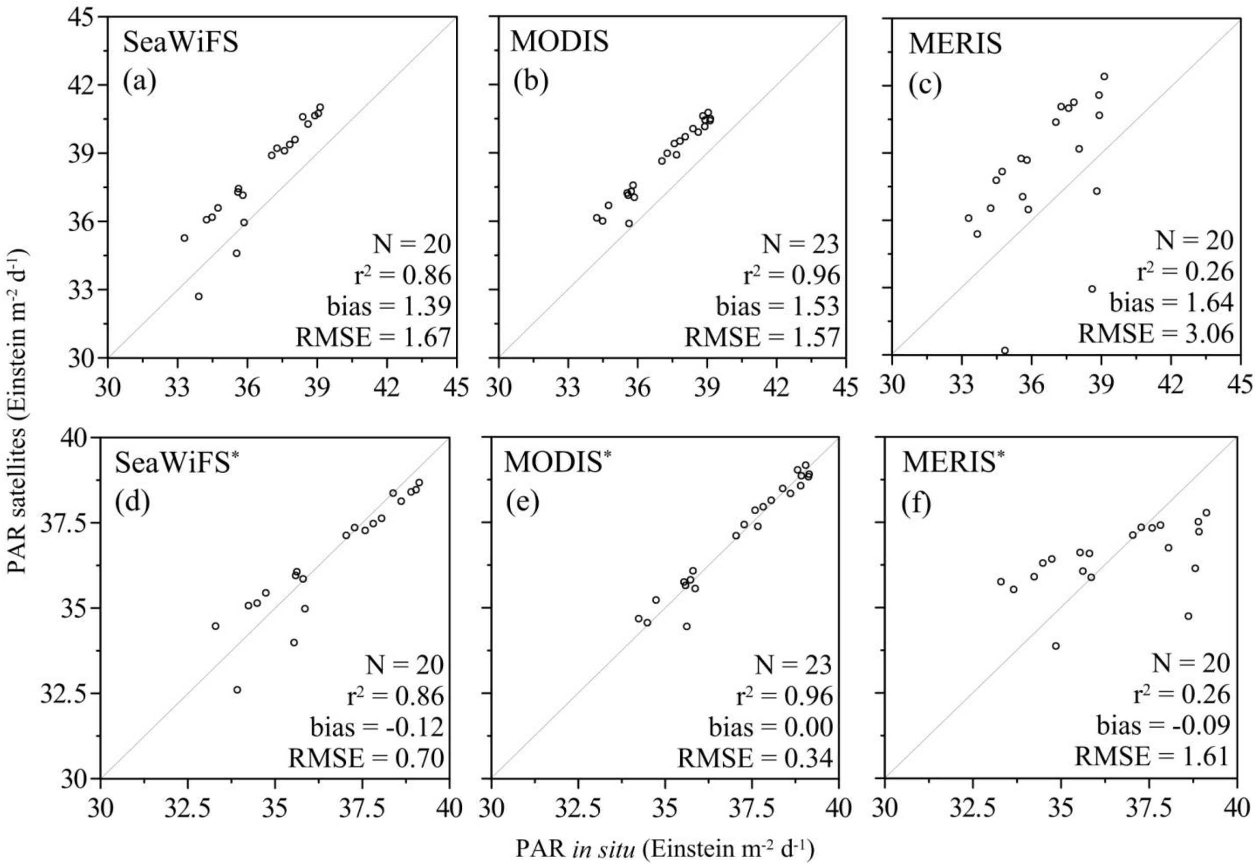

Figure 3. Scatterplots of daily PAR from *in situ* measurements and derived from non-adjusted SeaWiFS (a), MODIS-*Aqua* (b) and MERIS (c) data and adjusted ones (d, e, f).

Frouin et al. (2012) also analyzed the MODIS-*Aqua* algorithm and compared with SeaWiFS estimates. These authors obtained PAR overestimation for both sensors algorithms in relation to *in situ* measurements corroborating our present study. The performance of MODIS-*Aqua* and SeaWiFS were very close with MODIS-*Aqua* RMSE higher than SeaWiFS (difference ~0.27 Einstein m^{-2} d^{-1}) and with a lower bias (difference ~1.0 Einstein m^{-2} d^{-1}). Our present study showed an opposite pattern for MODIS-*Aqua* estimates compared to SeaWiFS (lower RMSE and higher bias) for non-adjusted algorithm. After the regional model adjustment the performance was better for MODIS-*Aqua* with lower values of RMSE and bias.

Dogliotti et al. (2014) observed a bias equal to 10 Einstein m^{-2} d^{-1} (~48%) with MODIS-*Aqua* data in the Argentine shelf (39°S to 55°S) and adjacent region during spring, late summer and late winter seasons. According to those authors although the bias had showed high values the PAR estimation had good r^2 in relation with *in situ* measurements explaining ~70% of variance (N = 36) suggesting that a GLM adjustment should be applied. A high estimate percentage error (5% to 73%) was observed by Vazyulya et al. (2016) using MODIS-*Aqua* daily PAR in comparison with *in situ* measurements made during a transit cruise from the Baltic to the White

Sea in the summer 2014. Laliberté et al. (2016) evaluated MODIS-*Aqua* Level-3 PAR at high northern latitudes and obtained a percentage error between 17% and 20%.

Our results for the winter cruise of 2002 showed a better performance when compared with other studies using data from the same sensors along the entire year. The performance of PAR estimates could perform better due to the less cloudiness during the winter in response to the seasonal rainy variation which predominates during summer (SANT'ANNA NETO, 2005). Also, typical lower SST values may reduce the evaporation and consequently the formation of clouds during the day resulting in better estimates from OCRS.

4. Conclusion

The present study showed a good agreement between PAR estimates and *in situ* measurements with more than 90% of accuracy. The observed performance of the PAR algorithm had an overestimation for the three sensors tested in our study region. The uncertainties may be due to cloud cover, atmospheric corrections, satellite's overpass time and sensor characteristics. A linear regression model was adjusted regionally correcting the observed systematic differences between the satellite PAR algorithm estimates and *in situ* measurements. The regional adjusted model effectively improved the estimation of PAR for SeaWiFS, MODIS-*Aqua* and MERIS data. Also, the GLM showed good performance when used in different seasons with SeaWiFS data. PAR estimates derived from other ocean colour sensors currently in operation such as Visible Infrared Imaging Radiometer Suite (VIIRS) and Ocean Land Colour Instrument (OLCI) should also be tested in the study region. The combination of geostationary and polar orbit satellites may allow to retrieve information about daily atmospheric changes decreasing the uncertainties associated with this parameter still present in current PAR algorithms and models.

Acknowledge

DEPROAS project was funded by CNPq/PRONEX-FINEP. Santos, J.F.C. had a MSc. scholarship from CNPq. This study was partially funded by the Inter-American Institute for Global Changes Research (US-NSF GEO-1128040 grant). The authors would like to thank the Ocean Biology Processing Group (OBPG) for SeaDAS and OCRS data distribution.

References

Antoine, D. Global-and ocean-scale primary production from satellite observations. In: GOWER, J. F. R. (ed). **Remote Sens. Mar. Environ**. 3. ed. Bethesda, MD: ASPRS pub. v. 6, p. 85–147, 2006.

Bird, R. E. A simple, solar spectral model for direct-normal diffuse horizontal irradiance. **Solar Energy**, v. 32, p. 461–471, 1984.

Denman, K. L. A time-dependent model of the upper ocean. **J. Phys.Oceanogr.**, v. 3, p. 173–184, 1973.

Dogliotti, A. I.; Lutz, V. A.; Segura, V. Estimation of primary production in the southern argentine continental shelf and shelf-break regions using field and remote sensing data. **Remote Sens. Environ.**, v. 140, p. 497–508, 2014.

Falkowski, P. G.; Laws, E. A.; Barber, R. T.; Murray, J. W. **Phytoplankton and their role in primary, new, and export production**. In: Fasham, M. J. R. (ed). Berlin, Heidelberg: Springer Berlin Heidelberg, c. 4, p. 99–121, 2003.

Falkowski, P. G.; Raven, J. A. **Aquatic photosynthesis**. Princeton, NJ: Princeton University Press, 2007.

Frouin, R.; Franz, B. A.; Werdell, P. J. **The SeaWiFS PAR product**. In: Patt, F. S.; Barnes, R. A.; Eplee, R. E.; Franz, B. A.; Robinson, W. D. (ed). Greenbelt, Maryland: NASA Goddard Space Flight Center, 2003. v. 22, Cap 8, p. 46–50, 2003.

Frouin, R.; McPherson, J.; Ueyoshi, K.; Franz, B. A. A time series of photosynthetically available radiation at the ocean surface from SeaWiFS and MODIS data. In: SPIE ASIA-2012, **Proceedings...** , 2012.

Frouin, R.; Pinker, R. T. Estimating photosynthetically active radiation (PAR) at the earth's surface from satellite observations. **Remote Sens. Environ.**, v. 51, n. 1, p. 98–107, 1995.

Gentemann, C. L.; Donlon, C. J.; Stuart-Menteth, A.; Wentz, F. J. Diurnal signals in satellite sea surface temperature measurements. **Geophys. Res. Lett.**, v. 30, n. 3, 1140, 2003.

Harmel, T.; Chami, M. Estimation of daily photosynthetically active radiation (PAR) in presence of low to high aerosol loads: application to OLCI-like satellite data. **Optics Express**, v. 24, n. 22, 2016.

IOCCG. Ocean-colour data merging. **Reports of the International Ocean Colour Coordinating Group,** n.6, p.74, 2007.

Kampel, M. **Estimativa da produção primária e biomassa fitoplanctônica através de sensoriamento remoto da cor do oceano e dados in situ na costa sudeste brasileira**. 2003. 279 p. Tese (Doutorado) - Universidade de São Paulo, Instituto Oceanográfico, São Paulo. 2003.

Kawai, Y.; Wada, A. Diurnal sea surface temperature variation and its impact on the atmosphere and ocean: a review. **Journal of Oceanography**, v. 63, p. 721–744, 2007.

Kirk, J. T. O. **Light and photosynthesis in aquatic ecosystems**. 3 ed. Orlando, Florida: Academic Press, p. 662, 1994.

Laliberté, J.; Bélanger, S.; Frouin, R. Evaluation of satellite-based algorithms to estimate photosynthetically available radiation (PAR) reaching the ocean surface at high northern latitudes. **Remote Sens. Environ.**, v. 184, p. 199–211, 2016.

Mobley, C. D.; Werdell, J.; Franz, B.; Ahmad, Z.; Bailey, S. Atmospheric correction for satellite ocean color radiometry. **A tutorial and documentation NASA ocean biology processing group**, p. 1–73, 2016.

Pereira, R. C.; Soares-Gomes, A. Produção primária marinha. In: **Biologia marinha**. Rio de Janeiro, RJ: Interciência, Cap. 10, 2002.

Sant'Anna Neto, J. L. Decálogo da climatologia do sudeste brasileiro. **Revista Brasileira de Climatologia**, v. 1, n. 1, p. 43–60, 2005.

Sathyendranath, S.; Platt, T. The spectral irradiance field at the surface and in the interior of the Ocean: a model for applications in Oceanography and Remote Sensing. **J. Geoph. Res.**, v. 93, p. 9270–9280, 1988.

Sigman, D.; Hain, M. The biological productivity of the ocean. **Nature education**, v. 3, n. 10, p. 21, 2012.

Vazyulya, S. V.; Kopelevich, O. V.; Sheberstov, S. V.; Artemiev, V. A. Estimation of sea surface solar radiation at 400-700 nm using satellite ocean color data, and its validation by ship data. **Optics Express**, v. 24, #254085, 2016.

Zege, E. P.; Ivaniv, A. P.; Katsev, I. L. **Image transfer through a scattering medium**. New York: Springer-Verlag, p. 349, 1991.